Symmetry boosts quantum computer performance

Y. S. Nam and R. Blümel

Department of Physics, Wesleyan University,

Middletown, Connecticut 06459-0155, USA

(Dated: January 28, 2016)

arXiv:1601.07497v1 [quant-ph] 27 Jan 2016

Abstract

Frequently, subroutines in quantum computers have the structure $\mathcal{F}\mathcal{U}\mathcal{F}^{-1}$, where $\mathcal{F}$ is some unitary transform and $\mathcal{U}$ is performing a quantum computation. In this paper we suggest that if, in analogy to spin echoes, $\mathcal{F}$ and $\mathcal{F}^{-1}$ can be implemented symmetrically such that $\mathcal{F}$ and $\mathcal{F}^{-1}$ have the same hardware errors on the logical qubit level, a symmetry boost in the fidelity of the combined $\mathcal{F}\mathcal{U}\mathcal{F}^{-1}$ quantum operation results that in our simulations reaches up to a factor 10. While we find and document this symmetry boost here in the case of Shor's algorithm, we suggest that other quantum algorithms might profit from similar symmetry performance boosts whenever $\mathcal{F}\mathcal{U}\mathcal{F}^{-1}$ sub-units of the corresponding quantum algorithm can be identified.

PACS numbers: 03.67.Lx

The second half of the 20th century saw the advent of the information technology revolution. There is no doubt about its profound impact on just about every aspect of modern society. The technological innovation in computers and networks enabled us to achieve tasks previously thought to be impossible, such as weather forecast, telecommunication, the Global Positioning System, and online banking.

While the current classical technology is already impressive, yet another revolution is about to emerge: Quantum information technology [1]. Taking advantage of quantum superposition and entanglement, a quantum information device is expected to be faster and more secure than its classical counterpart. Epitomizing this is Shor's algorithm [1, 2], which enables us to factor a semiprime $N = pq$, where p and q are prime numbers, exponentially faster than any classical algorithm known to date. Shor's algorithm is often associated with code-breaking since semiprime factorization is at the heart of the widely-employed Rivest-Shamir-Adleman (RSA) encryption algorithm [1, 3].

Despite all the theoretically predicted stupendous powers of quantum information devices, we do encounter major challenges when it comes to a physical realization of these devices: Errors and defects. This is so, because a quantum system is known to be susceptible to inexact manipulation and decoherence, especially for a quantum computer whose workings are based on exquisite control of quantum superposition and interference. An early list of the potentially dangerous physical mechanisms that may destroy the proper functioning of a quantum computer was compiled by Landauer [4], and much progress has been made to fight these detrimental mechanisms over the past couple of decades. For instance, overcoming the stochastic type of errors, i.e., errors that occur on a single qubit probabilistically, was the invention of quantum error correction [5–8] and its fault-tolerant implementation [9–11], culminating in the standard de facto approaches of topological and surface codes (see [12] and references therein).

Still, if we are to truly realize a working, physical quantum computer that is practically useful, the limits of engineering must be taken into consideration. Otherwise, a quantum computer will remain an academically interesting device of no practical relevance. One way to approach this problem is to investigate the accuracy gain in logical operations on a logical qubit, given the technology-dependent physical qubit error rate. Pioneering work in [13], for instance, is already making headway in this direction. Yet, another way to help realize the full potential of quantum computing is to investigate the algorithmic performance behavior

at the logical qubit level, providing quantum experimentalists and engineers with a logical error-rate target, potentially easing the accuracy and precision requirements. Adding to recent experimental breakthroughs, such as reported in [14] and [15], this paper provides an additional strategy for realizing a working, physical quantum computer.

As a testbed algorithm we chose Shor's algorithm, implemented according to Beauregard's architecture [16]. We selected this particular architecture based on the facts that (i) Shor's algorithm is arguably the most interesting and most important quantum algorithm to date, (ii) the algorithm is complex enough to realistically capture the effects of faulty gates, and, most importantly, and exploited in this paper, (iii) Beauregard's architecture allows us to take advantage of symmetry. Whether some other Shor algorithm architectures, such as those presented in [17] (and references therein), may be exploited in a similar fashion is currently under investigation and the results will be reported elsewhere.

Studies addressing the effects of errors and defects on a quantum computer running Shor's algorithm continue to be of central interest to many scientists. A list of early, notable contributions includes the investigations by Cirac and Zoller [18] studying the effect of errors in interaction time and laser detuning, Miquel *et al.* studying the effects of interactions with a dissipative environment [19] and phase drift errors [20], Wei *et al.* exploring the effects of coherence errors occurring while the quantum computer is idling [21], and García-Mata *et al.* simulating static imperfections in Shor's algorithm [22]. Recent developments in quantum simulation software [23, 24] reflect the fact that quantum computers remain at the forefront of research. Our work extends this line of research in that we simulate the entire Shor algorithm gate–by–gate. In particular, we investigate the effects of phase-rotation gate errors.

Since the most frequently used quantum gate in Beauregard's architecture of Shor's algorithm is a phase rotation gate

$$\theta_j^{(\pm)} = \begin{pmatrix} 1 & 0 \\ 0 & e^{\pm i\frac{\pi}{2^j}} \end{pmatrix}, \tag{1}$$

which appears $\sim 18L^4$ times throughout the algorithm [27] when using the minimally required number of qubits to factor a semiprime N whose bit-length is L, we tested the sensitivity of the quantum computer running Shor's algorithm with respect to effective errors introduced in $\theta_j^{(\pm)}$. Specifically, we used a statistical error model of the rotation gate

[26] of the form

$$ {}^{R}\theta_j^{(\pm)} = \begin{pmatrix} 1 & 0 \\ 0 & e^{\pm i\frac{\pi}{2^j}(1+\alpha^{(\pm)})} \end{pmatrix}, \tag{2} $$

in the case where the errors scale according to the size of the gate operation and

$$ {}^{A}\theta_j^{(\pm)} = \begin{pmatrix} 1 & 0 \\ 0 & e^{\pm i\left(\frac{\pi}{2^j}+\alpha^{(\pm)}\right)} \end{pmatrix}, \tag{3} $$

in the case where the errors do not scale according to the size of the operation. In both cases $\alpha^{(\pm)}$ is the defect parameter that may or may not be (strongly) correlated with the gate type indexed with j. In case a one-to-one correlation exists, we call the error "typed" and replace $\alpha^{(\pm)}$ with $\alpha_j^{(\pm)}$. The $\pm$ sign corresponds to forward and backward operation.

The reason why we investigate these two error models is as follows. First, any device has a finite accuracy, and this is usually given in terms of percentage error with respect to the size of the gate operation. Since a rotation gate θ_j is built according to a gate decomposition sequence (see references in [25]), together with the faulty logical gates, the approximated rotation gate will contain errors that scale in the size of the operation, especially regarding the construction method of θ_j by applying θ_{j+1} twice, for instance. This iteration method may be realistic and desirable from the technological or economical perspective. Thus, characterizing a device in terms of relative errors is captured by the ${}^{R}\theta_j^{(\pm)}$ model. However, suppose we characterize our quantum computer device in terms of its technological limit, say δ. In this case, most likely, all gates are to be made with different sequences resulting in an error level $\lesssim \delta$, and this is captured by our model ${}^{A}\theta_j^{(\pm)}$.

We now subdivide both models into 3 categories: (i) typed errors ($\alpha^{\pm} = \alpha_j^{\pm}$), asymmetric ($\alpha^{+} \neq \alpha^{-}$), (ii) typed errors ($\alpha^{\pm} = \alpha_j^{\pm}$), symmetric ($\alpha^{+} = \alpha^{-}$), and (iii) non-typed errors, i.e., completely random $\alpha^{\pm}$. The three categories are explained as follows. Typing arises from using the same sequence, or the same physical device, for the same θ_j that occur multiple times throughout the entire Shor algorithm. Then, depending on the way that the physical device is set up, since the backward gate is nothing but a unitary inverse of the forward gate, we may assume that the errors of the forward and backward gates are symmetric. Therefore, while (i) and (ii) capture systematic errors, (iii) deals with random errors.

To start with, we simulate the case of factoring $N = 15$. This is the case used in [20], which allows us to compare the results. Defining fidelity $F = |\langle\Psi_{\text{actual}}|\Psi_{\text{ideal}}\rangle|^2$ as in

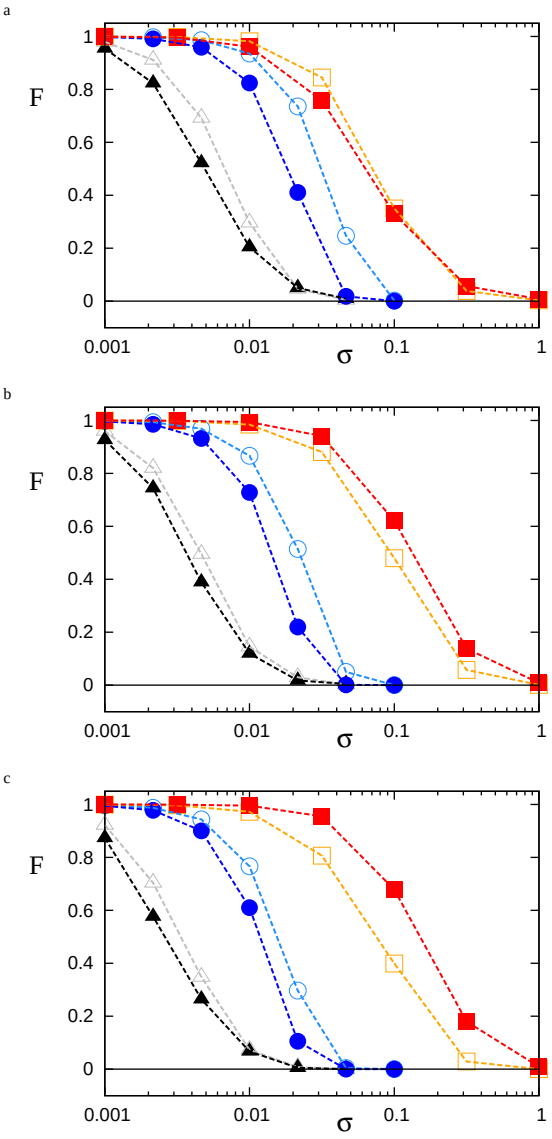

FIG. 1: Fidelity F of a quantum computer factoring $N = 15$ with seed 2 as a function of standard deviation σ of the logical-gate errors. In the order of a, b, and c, the quantum computer is equipped with adders that are capable of being used in Shor-algorithm-factoring of 4, 5, and 6-bit semiprimes. Shown are the cases of typed, asymmetric errors (triangles), typed, symmetric errors (squares), and non-typed, random errors (circles). Filled plot symbols (Red, Blue, and Black) denote relative errors [see Eq.(2)] and the open plot symbols (Orange, Cyan, and Grey) denote absolute errors [see Eq.(3)]. Dashed lines connecting plot symbols are drawn to guide the eye. The solid, horizontal lines correspond to $F = 0$.

[20], in Fig. 1 we plot F as a function of σ, where the errors $\alpha^{(\pm)}$ are Gaussian distributed random variables with mean 0 and standard deviation σ. At first glance, we observe that the quantum computer performs better in the order of the asymmetric, random, and symmetric errors. In particular, symmetric errors give rise to a fidelity boost in σ by an astonishing factor of ~ 10 in both the ${}^{R}\theta_j^{\pm}$ and the ${}^{A}\theta_j^{\pm}$ models.

To better feature the symmetry-driven fidelity boost, this time we plot, in Fig. 2a, the fidelity F of Shor's algorithm as a function of the number of qubits n, while fixing the error strength $\sigma = 10^{-8/3}$, $10^{-6/3}$, and $10^{-4/3}$ for asymmetric, random, and symmetric errors, respectively. The error strengths were chosen so that the corresponding resulting fidelities are roughly of the same magnitude, pointing to the fact that there exists a fidelity boost due to symmetry. A surprising result: Not only does the fidelity boost persist, but the boost is in fact enhanced as a function of increasing n. While one may expect that the fidelity should decrease for increasing n (after all, the quantum computer is exposed to a larger number of erroneous gates), for the symmetric case, apparently, there is an anomalous initial *increase* in F.

In an attempt to find the scaling relation of F for Shor's algorithm as a function of σ and n, we now probe a smaller computational unit of Shor's algorithm. In Figs. 2b and c, we plot the fidelity F of a U-gate as a function of the bit-length L of the adder, equipped with uncorrelated relative and absolute errors, respectively (as shown in [16], a U-gate is a multiplier gate, i.e., a computational unit one level smaller than a full modulo-exponentiation gate). Numerically we find that the U-gate fidelities for both cases are Gaussian in both σ and L (see caption of Fig. 2 for details). The results are in excellent agreement with the corresponding data in Fig. 1 and Fig. 2a, obtained by multiplying a factor $2L$ to the exponent of the U-gate scaling relations (not shown), reflecting the fact that there are $2L$ U-gates in a complete modulo-exponentiation circuit in Shor's algorithm. For reference we note that, according to [16], $n = 4L + 3$.

While similar behavior is observed for the interesting symmetric cases at the U-gate level, currently no explicit formula is available. At present, it is sufficient to note that, for a given L, the U-gate fidelity is (i) Gaussian in σ for small σ and (ii) exponential in σ for large σ. Explicit numerical computations show that the scaling parameters are sensitive to both the multiplier of a U-gate and the semiprime N. An additional difficulty arises in predicting the fidelity scaling of the entire Shor algorithm: The technique of multiplying a factor $2L$

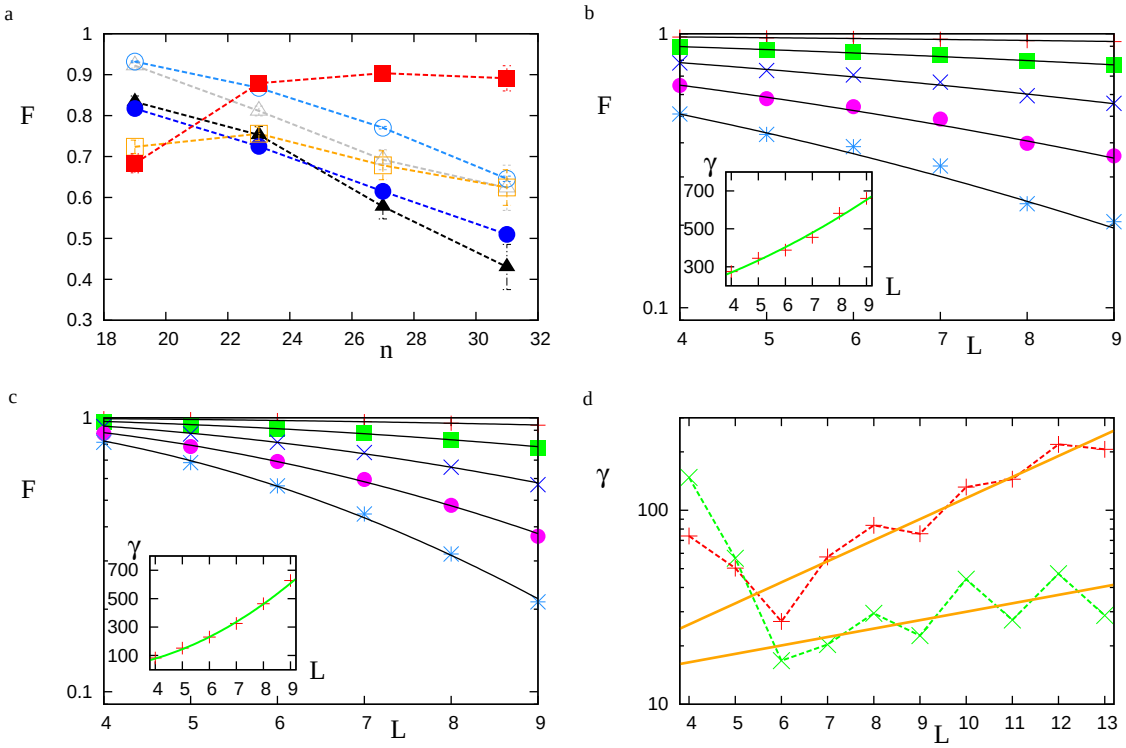

FIG. 2: Fidelity F of Shor's algorithm running in various modes. Frame a: Factoring 15 with seed 2 with $n = 19, 23, 27$ and 31 qubits, where $\sigma = 10^{-8/3}, 10^{-6/3}$, and $10^{-4/3}$ for asymmetric (triangles), random (squares), and symmetric (circles) errors, respectively. Frames b and c: Fidelity F of a U-gate (see [16]) computing the controlled modulo-multiplication $2 \times 1 \bmod 15$ with the control qubit turned on (qubit state $|1\rangle$), as a function of adder size L, defined as the maximal bit-length of a semiprime that may be factored when the adder is used in Shor's algorithm. The U-gates are equipped with adders that contain random errors (b: relative and c: absolute). Shown are the cases with $\sigma = 0.01$ (pluses/red), $\sigma = 0.02$ (squares/green), $\sigma = 0.03$ (crosses/blue), $\sigma = 0.04$ (circles/purple), and $\sigma = 0.05$ (asterisks/cyan). Black lines are fit-lines of the form $\exp\left[-10(L+5)^2\sigma^2/3\right]$ and $\exp\left[-10(L-1.2)^2\sigma^2\right]$ for Frames b and c, respectively. Insets in Frames b and c show γ, defined according to $F = \exp[-\gamma(L)\sigma^2]$, for $\sigma = 0.01$ as a function of L. Frame d: An equivalent plot to the insets in Frames b and c for symmetric errors. Pluses (red) and crosses (green) are absolute and relative errors, respectively. Dashed lines guide the eye. The fit functions (orange solid lines) for the tail regions are $\exp[(L+9)/4]$ and $\exp[(L+24)/10]$ for absolute and relative errors, respectively.

to the exponent of the U-gate fidelity scaling fails. A pleasant surprise, on the other hand, is the following: The true Shor fidelity outperforms expectations.

Remaining in the small-σ regime [case (i)], important for practical applications, and assuming the functional form $\exp(-\gamma\sigma^2)$ of the fidelity of the U-gate equipped with correlated, symmetric noise, we extract the coefficient γ and plot it against L in Fig. 2d. Consistent with earlier observations, the U-gate initially performs better as a function of increasing L, reverting to the expected behavior of deteriorating fidelity for $L > L_c$. While the exact scaling relation of L_c is currently unknown and forms a topic for future investigations, in the remaining part of the paper, we turn to a more important question: Is the symmetry-driven fidelity boost persistent in n (and/or L)?

Tracking down the origin of the anomalous behavior, we first tested various computational sub-units of Shor's algorithm. We find that a modulo-addition gate is the smallest unit that exhibits the symmetry-driven fidelity boost. In Fig. 3a and b, we plot the fidelity F of the modulo-addition gate, equipped with the typed, symmetric, relative and absolute errors, respectively, executing $0+2 \bmod 15$ as a function of the bit-length L of the adder for various error levels σ. We observe that both types of errors result in an initial boost in fidelity, followed by deterioration. We note that while the relative kind of errors shows sustained deterioration of F in L, as would be expected from further introducing relatively more noisy gates, the absolute kind of errors nearly plateaus out. This may be explained as follows. While the absolute kind of noise may drown out the rotation gates with rotation angles smaller than the noise amplitude, it leaves those with angles larger than the noise amplitude relatively unaltered, effectively keeping the hierarchy of rotation angles (i.e. $\theta_{j+1} < \theta_j$) intact. This observation agrees with the findings in [28], i.e., banding and hierarchy in certain quantum circuits, such as in the quantum Fourier transform (a backbone subroutine of Shor's algorithm [16]), are the determining factors of the performance of a quantum computer.

We now turn to the question of persistence of the symmetry-induced performance boost for different semiprimes. So far, we have used $N = 15$ as our test case. The question now is whether for all other N's the performance boost continues to be observed. In particular, we are interested in how the fidelity changes when additional qubits are introduced into the modulo-addition gate. To this end, we numerically simulated $0 + 2 \bmod N$ for all odd semiprimes $N < 2^{13}$ with 0, 1, 2, and 3 additional qubits in the modulo-addition gate and

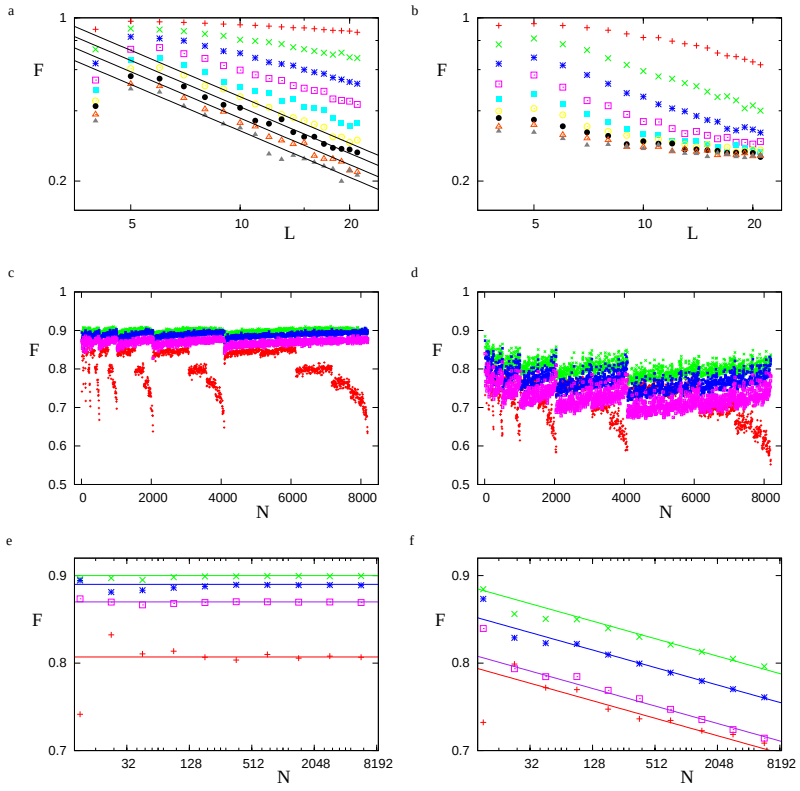

FIG. 3: Fidelity F of a modulo-addition gate performing $0+2 \bmod N$, where N is a semiprime. Frames a and b show F as a function of the bit-length L of the maximal semiprime that may be factored using the employed modulo-addition gate, equipped with relative and absolute symmetric errors, respectively. All cases were performed with $N = 15$. In decreasing order of F, different plot symbols refer to $\sigma = 0.1, 0.2, \ldots, 0.9$. The solid black lines in Frame a are the large-L regime fit-lines $(2\sigma+0.3)^{-2/3}$ for $\sigma \geq 0.6$. Frames c and d show F as a function of all odd semiprimes $N < 2^{13}$ for relative and absolute symmetric errors, respectively. The error strength used is $\sigma = 0.2$. In the order of pluses (red), crosses (green), asterisks (blue), and squares (purple), the adders are equipped with 0, 1, 2, and 3 additional qubits than minimally required. Frames e and f show logarithmically averaged F, i.e., each plot point at x-coordinate of $2^{j+1/2}$ is the result of averaging over N from 2^j to 2^{j+1}, where $3 \leq j \leq 12$. Notice that for $j = 3$ and $j = 4$, there is only one semiprime each, namely, 15 and 21, respectively, resulting in larger fluctuations due to insufficient statistics. Solid lines in Frame e, with corresponding color symbols, are the tail-region fit lines $F = 0.807, 0.9, 0.89,$ and 0.87. Solid lines in Frame f, with corresponding color symbols, are the tail-region fit lines (to first order) $F = -0.01 \log_2(N) + k$, where $k = 0.827, 0.918, 0.885,$ and 0.841 for the four cases shown.

plot the resulting F as a function of N in Fig. 3 c and d for the relative and absolute cases with $\sigma = 0.2$, respectively. Clearly, we see that for all semiprimes we tested, there is an apparent fidelity boost for both relative and absolute errors. Another interesting phenomenon is that semiprimes N between 2^j and 2^{j+1} are sectioned into different F-bands, probably arising from the bit-spectra of different N values, i.e., the binary digit 1 in the digit spectrum of N turns on the corresponding noisy rotation gate operation. This, however, forms a subject of research in itself and is beyond the scope of this paper.

To highlight the result shown in Fig. 3 c and d, we averaged F over N in logarithmic scale, i.e., $2^j < N < 2^{j+1}$ for $j = 3, 4, \ldots, 12$, and plot the results in Fig. 3 e and f, respectively. We immediately confirm that the performance boost persists. In addition, we see that (A) the fidelity does not scale in N for the relative type of noise and (B) the fidelity does scale in N, like $\sim \log_2(N)$, for the absolute type of noise. While the exact reasoning behind these two observations is currently unknown, on the basis of the following two arguments we speculate that (A) and (B) are direct consequences of the hierarchical structure competing with the fixed-strength errors. First, additional qubits used in the modulo-addition gates correspond to increasing the depth of the hierarchy of the quantum gates, which helps increase F in the absence of errors. Then, for a fixed-strength error $\sigma > 0$, the relative kind affects the entire hierarchy of the modulo-addition gates evenly, i.e., all constituent rotation gates of the modulo-addition gates are subjected to the same relative strength of errors. This results in the plateau behavior of F as shown in Fig. 3 e. In contrast, the absolute kind of errors drowns out all rotation gates with rotation angles less than the noise level, which necessarily comes about as N increases. This is consistent with the scaling of F in $\log_2(N) \sim L$ (see Fig. 3 f) in that the number of drowned-out gates scales in L as well.

While we conjecture that the symmetry boost presented in this paper persists in the regime of a large number of qubits, we were able to check this explicitly only for $n \leq 31$. Going beyond, however, becomes prohibitively expensive, taking into account that a large number of runs are needed to gather statistics. For instance, let us take a look at memory requirements. With double-precision complex numbers, a single run of the n-qubit case requires at least 2^{n-26} GB of RAM, which already for $n = 300$ (a relatively small number of qubits in view of practical applications), amounts to more than 10^{80} GB, which exceeds the classical resources of the entire known universe. Together with a runtime that is exponential in n, any classical computer, present or future, quickly reaches its limits. Nonetheless, on

the basis of the simple analytical scaling formula found in Fig. 2, we arrive at the prediction that factoring a 1000-bit semiprime with $\sim 40\%$ fidelity would require error levels of the order of $\sim 10^{-3}\,\%$ for uncorrelated noise, perfectly within practical engineering limits.

The error-level requirement is relaxed further when the noise becomes symmetric. In fact, as shown in Fig. 1 and Fig. 2 a, for factoring $N = 15$, more than a factor of 10 in σ of symmetric noise is allowed for a fidelity comparable to what would be observed in the uncorrelated cases. In fact, we numerically confirm that the fidelity of modulo-addition gates exposed to relative, uncorrelated noise scales like $\exp(-1.73L)$, consistent with the fidelity scaling we obtained from Fig. 2 since there are $2L$ modulo-addition gates in a single U-gate. Together with the findings in Fig. 3, i.e., that the fidelity of modulo-addition gates subjected to symmetric noise is approximately constant in L when compared to its uncorrelated counterparts, we arrive at the conclusion that symmetric noise effectively lowers the power of L in the exponent of the fidelity scaling relations of Shor's algorithm that are subjected to the uncorrelated noise. Fidelity may be further enhanced by employing extra qubits in the adder. According to Fig. 3, this "trick" will result in a constant boost in F for the modulo-addition gates, ultimately decreasing the coefficients in the exponent. Assuming (i) that for small σ the modulo-addition gates are operating with near perfect fidelity and (ii) that the Shor fidelity, to a good approximation, may be obtained by multiplying the modulo-addition gate fidelity by the number of its occurrences, denoting by δ and Δ the differences of fidelity from 1 of the modulo-addition gates with and without additional qubits, respectively, we obtain for $\delta < \Delta$ a reduction in the coefficient of the exponent by approximately δ/Δ. At this point, we recall that Shor's algorithm with symmetric noise performs better than expected on the basis of naive multiplication of the fidelities of its corresponding smaller computational sub-units. Therefore we conclude that our findings are a lower bound of the ultimately achievable improvement in fidelity, since other parts of the algorithm may be identified which may also be implemented symmetrically with an accompanying additional boost in fidelity.

We are certain that our results are a welcome boon for quantum experimentalists and engineers. Not only is the quantum computer already resilient against irremovable hardware errors, but, as we showed in this paper, exhibits significant performance enhancement just by controlling the symmetry of the errors. We also showed that using symmetry as a method to boost performance is well within engineering capabilities. This is supported by the fact

that spin-echoes [29], e.g., already proved useful for practical applications in suppressing the naturally occurring errors in a given physical system. While it is still true that the symmetry needs to be implemented to a high precision, from the engineering perspective, the task of keeping the symmetry should be easier than keeping the error level itself small. Our results are also of interest to theorists. Given that the symmetry was the key for the dramatic fidelity boost at the architectural, surface level, as opposed to the individual, microscopic, inner-workings of a single-qubit state, we gain the insight that a topologically and structurally robust quantum algorithm may be developed. Given the fact that quantum algorithms, in general, tend to contain a large number of symmetric structures, we expect that designing hardware that results in symmetric errors, as exploited in this paper, may be beneficial for boosting performance in other quantum algorithms as well.

It would have been lamentable if the irremovable hardware errors in the logical qubits proliferated too quickly for a quantum computer to be of practical use. Fortunately, as we showed in this paper, this is not so. Together with the pioneering works in quantum error correction and its fault-tolerant implementation, the surprising robustness of quantum computers with respect to errors and noise suggests that quantum computing and quantum information is not just of academic interest but is practically useful and important.

ADDITIONAL INFORMATION

Competing financial interests: The authors declare no competing financial interests.

[1] Nielsen, M. A. & Chuang, I. L. *Quantum Computation and Quantum Information* (Cambridge Univ. Press, 2000).

[2] Shor, P. W. *Proc. 35th Annual Symp. Foundations of Computer Science* 124-134 (IEEE, 1994).

[3] Rivest, R., Shamir, A., & Adleman, A. A method for obtaining digital signatures and public-Key cryptosystems. *Comm. ACM* **21** (2), 120-126 (1978).

[4] Landauer, R. *Quantum Computing and Communications*, edited by M. Brooks (Springer, 1999), 61.

[5] Shor, P. W. Scheme for reducing decoherence in quantum computer memory. *Phys. Rev. A* **52** R2493-R2496 (1995).

[6] Steane, A. M. Error correcting codes in quantum theory. *Phys. Rev. Lett.* **77**, 793-797 (1996).

[7] Calderbank, A. R. & Shor, P. W. Good quantum error-correcting codes exist. *Phys. Rev. A* **54**, 1098-1105 (1996).

[8] Laflamme, R., Miquel, C., Paz, J. P. & Zurek, W. H. Perfect quantum error correcting code. *Phys. Rev. Lett.* **77** 198 (1996).

[9] Shor, P. W. *Proc. 37th Annual Symp. Foundations of Computer Science* 56-65 (IEEE,1996).

[10] Steane, A. M. Fault-tolerant quantum computing. *Nature* **399**, 124-126 (1999).

[11] Gottesman, D. Theory of fault-tolerant quantum computation. *Phys. Rev. A* **57**, 127-137 (1998).

[12] Fowler, A. G., Mariantoni, M., Martinis, J. M. & Cleland, A. N. Surface codes: Towards practical large-scale quantum computation. *Phys. Rev. A* **86**, 032324 (2012).

[13] Fowler, A. G., Whiteside, A. C., McInnes, A. L. & Rabbani, A. Topological code Autotune. *Phys. Rev. X* **2**, 041003 (2012).

[14] Barends, R. *et al.* Superconducting quantum circuits at the surface code threshold for fault tolerance. *Nature* **508**, 500-503 (2014).

[15] Muhonen, J. T. *et al.* Storing quantum information for 30 seconds in a nanoelectronic device. *Nat. Nanotech.* **9**, 986-991 (2014).

[16] Beauregard, S. Circuit for Shor's algorithm using 2n+3 qubits. *Quantum Inf. and Comput.* **3**, 175-185 (2003).

[17] Markov, I. L. & Saeedi, M. Constant-optimized quantum circuits for modular multiplication and exponentiation. *Quantum Inf. Comput.* **12**, 361-394 (2012).

[18] Cirac, J. I. & Zoller, P. Quantum computations with cold trapped ions. *Phys. Rev. Lett.* **74**, 4091-4094 (1995).

[19] Miquel, C., Paz, J. P. & Perazzo, R. Factoring in a dissipative quantum computer. *Phys. Rev. A* **54**, 2605-2613 (1996).

[20] Miquel, C., Paz, J. P. & Zurek, W. H. Quantum computation with phase drift errors. *Phys. Rev. Lett.* **78**, 3971-3974 (1997).

[21] Wei, L. F., Li, X., Hu, X. & Nori, F. Effects of dynamical phases in Shor's factoring algorithm with operational delays. *Phys. Rev. A* **71**, 022317 (2005).

[22] García-Mata, I., Frahm, K. M. & Shepelyansky, D. L. Shor's factorization algorithm with a single control qubit and imperfections. *Phys. Rev. A* **78**, 062323 (2008).

[23] Wecker, D. & Svore, K. M. LIQUi|>: A software design architecture and domain-specific language for quantum computing. Preprint at http://arxiv.org/abs/1402.4467 (2014).

[24] García, H. J. & Markov, I. L. Simulation of quantum circuits via stabilizer frames. *IEEE Trans. on Comput.* **64**, 2323-2336 (2014).

[25] Nam, Y. S. & Blümel, R. Performance scaling of the quantum Fourier transform with defective rotation gates. *Quantum Inf. Comput.* **15**, 721-736 (2015).

[26] Nam, Y. S. & Blümel, R. Robustness of the quantum Fourier transform with respect to static gate defects. *Phys. Rev. A* **89**, 042337 (2014).

[27] Nam, Y. S. & Blümel, R. Robustness and performance scaling of a quantum computer with respect to a class of static defects. *Phys. Rev. A* **88**, 062310 (2014).

[28] Nam, Y. S. & Blümel, R. Structural stability of the quantum Fourier transform. *Quantum Inf. Process.* **14**, 1179-1192 (2015).

[29] Hahn, E. L. Spin echoes. *Phys. Rev.* **80**, 580-594 (1950).

AUTHOR CONTRIBUTIONS

Y. S. Nam and R. Blümel devised the idea and wrote the main manuscript. Y. S. Nam analyzed the results.